

3 (VIBE) MR : 가 1

. 2 .

: 가 (volume interpolated breath - hold examination;
3D - VIBE) 3 (Magnetic Resonance
Imaging: MRI) 2 MRI . 23
:
25 1.5T MR . 20 mL 가
(Gd - DTPA) 3 mL 3 VIBE
T1 , 3 VIBE 2
(2 - dimensional fast low angle shot, 2D - FLASH) T1
2D - FALSH .
,
,
가 . , (maximum intensity projection:
MIP) 3D - VIBE MR
:
2D FLASH 3D VIBE
3D - VIBE 2D - FLASH
($p > .05$). 2D - FLASH 3D -
VIBE ($p < .05$).
3D - VIBE , 2D - FLASH 2D - FLASH
, 2D - FLASH 가 ($p < .05$).
3D - VIBE 2D - FLASH
3D - VIBE 2D - GRE ($p < .05$).
VIBE MIP
,
: 3D - VIBE 2D - FLASH ,
2D - FLASH MR .

(Magnetic reso - (1, 2).
nance imaging: MRI) CT

, CT 가 (3 - 5),
가,
가 (6,
, CT
MRI

2002 8 16

2002 11 16

가 , 가 MRI (Gradient echo: 2D - GRE) 가 (10 - 13). 2D - GRE (volume averaging effect) (14). 3 MR (gradient echo: 3D - GRE) (15 - 17). 2D - GRE reformation, MPR) MIP 3D - GRE MR 가 3D - VIBE MR 2 MR (2001 1 2002 5 MRI 23 25 35 81 , 53.2 17:6 , 16 , 1 , (Malignant fibrous histiocytoma, MFH) 1 , 1 , 6 . 25 가 9 , 14 1 . 1 - 14 cm 5.34 cm . 12 13 , CT, MR 6 (1.5 T (Magnetom Symphony; Siemens, Enlargen, Germany) (phased array multicoil) (VIBE) T1 2 FLASH 3 VIBE TR/TE=120/2.6, (flip angle) 70 , 7 mm 20 - 25 . 3 VIBE TR/TE=3.4 - 3.8/1.4 - 1.8, 12 , (Bandwidth) 490 Hz/ , (partition number) 48 - 52, (matrix size) 121 × 256, (effective slice thickness) 2.0 - 2.6 mm , (Field of view) 38 cm, 18 - 20 . , 33 cm, 2.3 mm, 64 - 72 . (volumetric inter - polation) (Kz) 69%, 82% (sampling) (interpolation) 6/8 . 3 VIBE (source) MR workstation 5 - 8 mm . Gd - DTPA (Magnevist, Scherring, Berlin, Germany) 1 ml 10 ml (test bolus technique) . 19 ml 3 ml (automatic injector) , 10 ml 가 . (VIBE 25 (nephrogram phase) 가 3 2D - FLASH 4 3D - VIBE . , 3 cm (MR Urography, MRU) (Lasix 20 mg, Handok, Seoul, Korea) VIBE 가 . 2D - FLASH 3D - VIBE (Region of interest, ROI) . ROI (phase encoding direction) (signal to noise ratio: SNR) (contrast noise ratio: CNR) 1.5 T (Magnetom Symphony; Siemens, Enlargen, Germany) (phased array multicoil)

: ROI

2 가 2D - FLASH 2D - FLASH 3D - VIBE
 3 4 2D - FLASH 2D - FLASH SNR 2D - FLASH
 3D - VIBE 1) 2) 3) SNR 2D - FLASH
 2) 3) 4) 1 - 4 (:1, 2D 3D
 2, 3, 4) 1 - 4 2D FLASH 2D FLASH
 가 1 가 1 (Table 1). 가 3D - VIBE (3.84
 가 2 , 가 3 , 가 2D - FLASH (3.36 ± 0.64)
 4 2D - FLASH (3.33 ± 0.56) (p < .05),
 1 , 2D - FLASH (2.58 ± 0.72)
 가 2 , 가 2D - FLASH (3.04 ± 0.61) 3D - VIBE
 3 . (3.88 ± 0.33) (Table 2).
 4 3D - VIBE 2D - FLASH
 MIP (MR 2D - FLASH (p < .05).
 angiography; MRA) 3D - VIBE (3.68 ± 0.48) 2D - FLASH

Table 1. Results of Quantitative Analysis: SNR and CNR of 25 Renal Tumors in Three Imaging Techniques

	Pre-contrast 2D FLASH	Post-contrast 2D FLASH	Post-contrast 3D VIBE	P-value
SNR _{kidney}	15.92	37.68*	46.72*	p < .05
SNR _{mass}	11.94	23.61*	22.39*	p < .05
CNR _{renal mass}	- 3.98	- 14.07	- 24.33 [†]	p < .05

Data are given as mean values.

* Mean tumor and renal parenchymal SNR of post-contrast 2D-FLASH and 3D-VIBE images were higher (p < .05) than that of pre-contrast 2D-FLASH image. No significant differences (p > .05) in tumor and renal parenchymal SNR between post-contrast 2D-FLASH and 3D-VIBE images.

[†]The CNR of 3D-VIBE image is significantly higher than that of other images (p < .05).

Table 2. Results of Qualitative Analysis: Subjective Image Parameters of Three Imaging Techniques

	Pre-contrast 2D FLASH	Post-contrast 2D FLASH	Post-contrast 3D VIBE	P-value
General quality	3.36 ± 0.64	3.33 ± 0.56	3.84 ± 0.37*	p < .05
Artifacts	3.04 ± 0.61	2.58 ± 0.72	3.88 ± 0.33*	p < .05
Lesion Conspicuity	2.00 ± 0.58	3.54 ± 0.59 [†]	3.68 ± 0.48 [†]	p < .05
Lesion Delineation	2.40 ± 0.82 [‡]	3.29 ± 0.55 [‡]	3.80 ± 0.40 [‡]	p < .05

Data are the mean ± standard deviation.

* Post-contrast 3D-VIBE image have higher image quality and lower artifacts than 2D-FLASH images (p < .05).

[†] Post-contrast 3D-VIBE and 2D-FLASH images have a significant difference with precontrast 2D-FLASH image (p < .05).

[‡] The difference among the each images obtained with three imaging techniques is significant (p < .05).

(3.54+ - 0.59)
 ($p > .05$), 3D - VIBE
 (3.80+ - 0.40) 2D - FLASH (3.29+ - 0.55)
 ($p < .05$)(Fig. 1).
 MRA
 2

(VIBE)
 가 1 가 . 16
 MIP 7 (47%) . 23 MIP 17
 가 MIP
 가

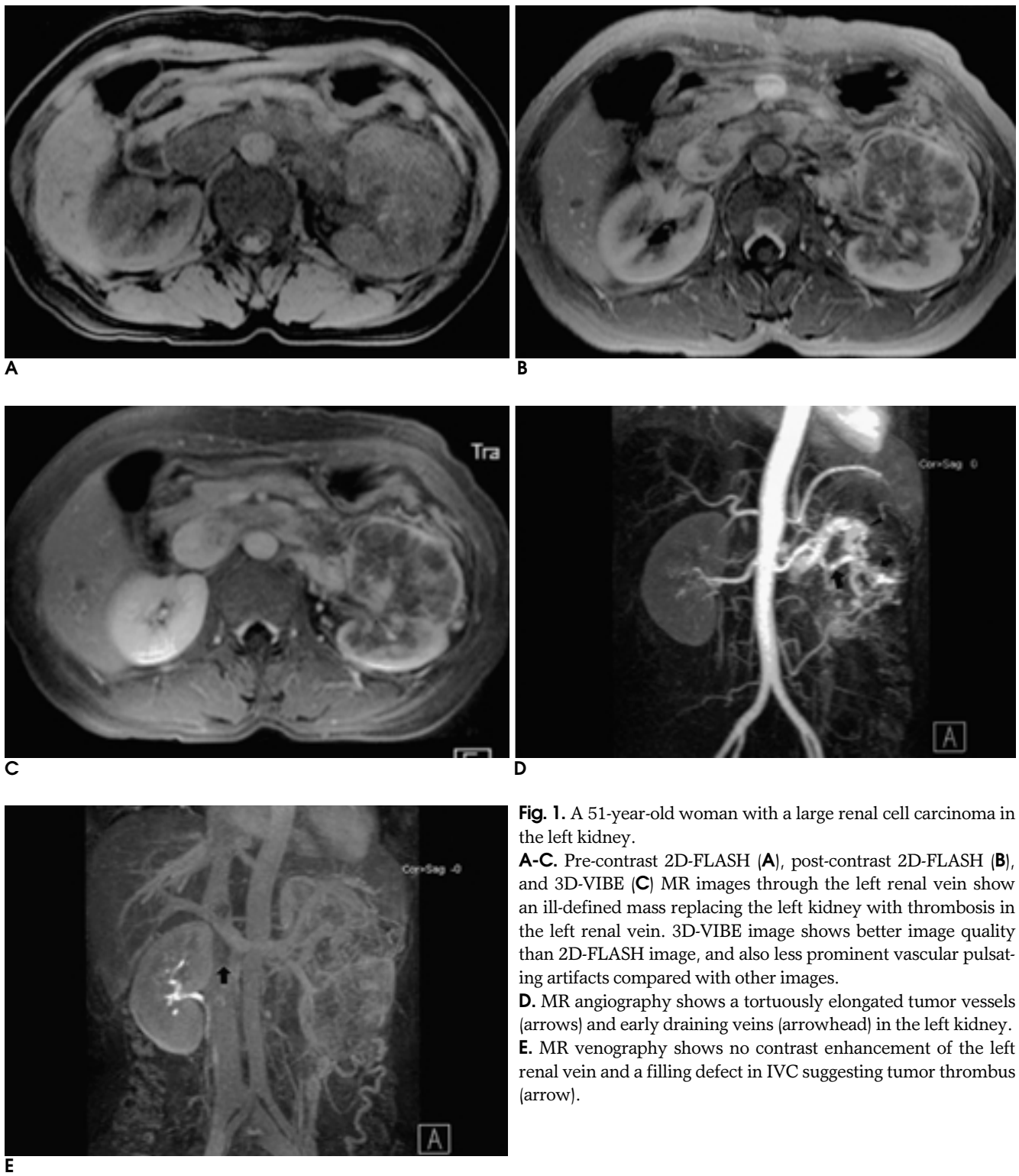


Fig. 1. A 51-year-old woman with a large renal cell carcinoma in the left kidney.
A-C. Pre-contrast 2D-FLASH (**A**), post-contrast 2D-FLASH (**B**), and 3D-VIBE (**C**) MR images through the left renal vein show an ill-defined mass replacing the left kidney with thrombosis in the left renal vein. 3D-VIBE image shows better image quality than 2D-FLASH image, and also less prominent vascular pulsating artifacts compared with other images.
D. MR angiography shows a tortuously elongated tumor vessels (arrows) and early draining veins (arrowhead) in the left kidney.
E. MR venography shows no contrast enhancement of the left renal vein and a filling defect in IVC suggesting tumor thrombus (arrow).

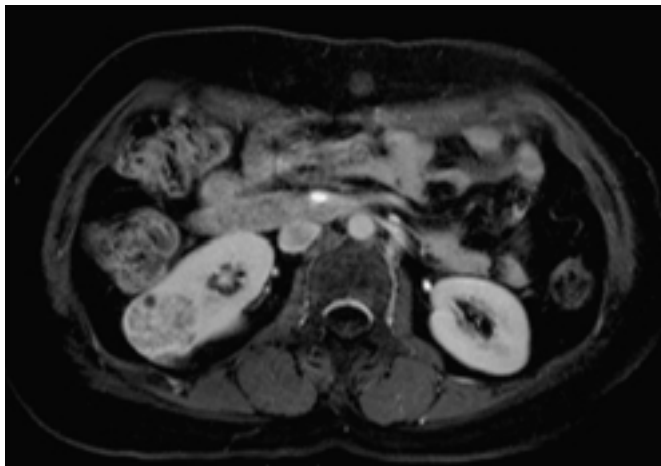
MIP
6 (40%)
(Fig. 1). MIP
, MRI
6
가 MRU
가 11 (50 %),
가 2 (9%),

가 6 (23%),
가 4 (18%) . MRU
가
(Table 3). 23
가 3 cm
가
가
(Fig. 3).

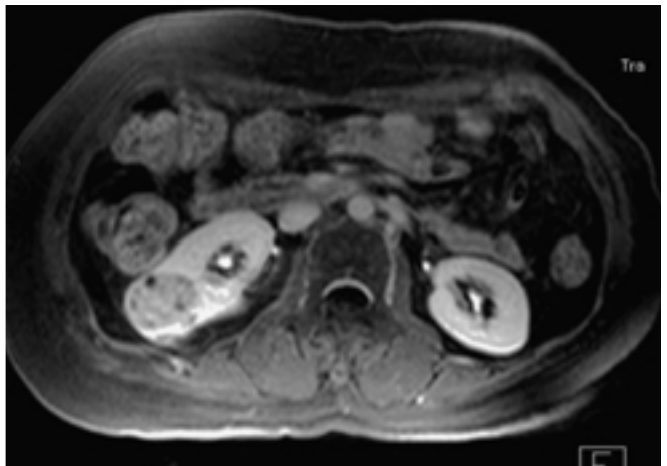
Table 3. Pelvocalyceal Delineation of 23 Patients with Renal Masses on Magnetic Resonance Urography

Delineation of pelvocalyceal system	No of Patients	Mean mass size (cm)
Normal pelvocalyceal system	11 (48%)	2.7
Involvement of renal calyx	2 (9%)	6.5
Involvement of renal pelvis or hydronephrosis	6 (26%)	9.2
No visualization of renal pelvocalyceal system	4 (17%)	9

가 MRI
,
CT
(8, 10).
MRI
가
2D - GRE



A



B

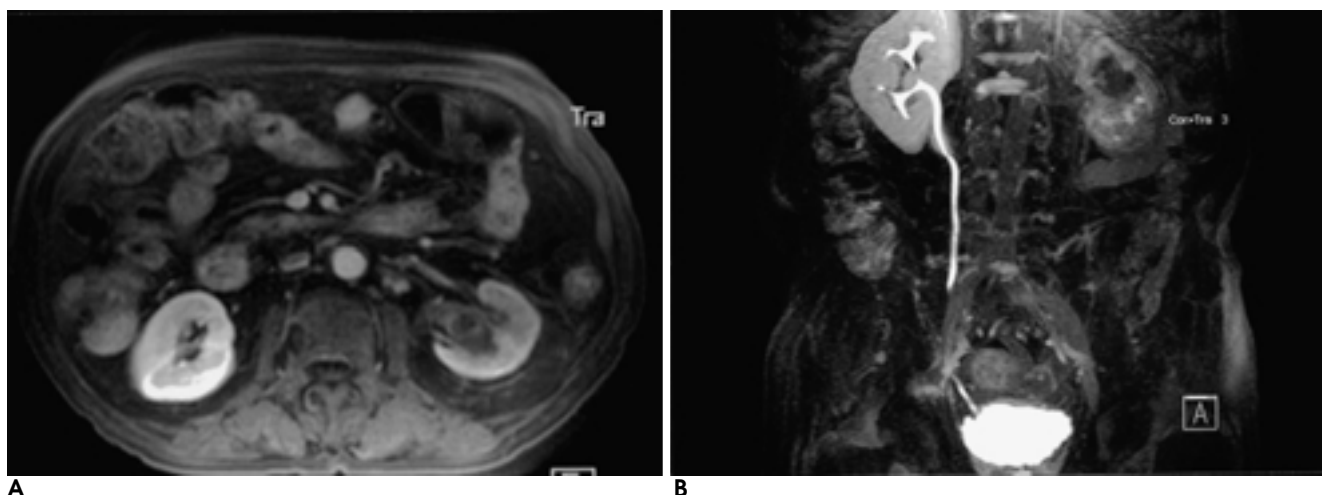


C

Fig. 2. A 51-year female with a 3-cm sized renal cell carcinoma in the right kidney.

A, B. Post-contrast 2D-FLASH (**A**), and post-contrast 3D-VIBE (**B**) MR image shows a well defined heterogeneously enhancing mass in the right kidney.

C. MR urography shows a good depiction of renal pelvocalyceal system as well as the tumor.



A **B**

Fig. 3. A 78-year old man with a transitional cell carcinoma in the left kidney.

A. Post-contrast 3D-VIBE Image shows a heterogeneously enhanced small mass in the left renal pelvis.

B. MR Urography shows no excretion of contrast material into the left urinary tract due to long-standing obstruction of the renal pelvis by tumor.

(19). , (p < .05). , VIBE 가 , (voxel) (14). 3D - GRE MR 가 (14, 18). 2D - GRE 가 (16). 3D - , 3D - VIBE , MIP 가 가 . (15, 16, 20). , (Radiofrequency thermal ablation) (22, 23), 3D - GRE 가 가 3 mm (6, 7, 17, 24). MIP MR 3D - GRE VIBE 120 MRA 가 , 3 cm MRU (21). , VIBE 2D - GRE 2D - GRE 2 - 3 (1) 가 가 . 2D - GRE 가 가 2 - 2.3 mm 640

가 가 가 .

, , VIBE

18 mm 50 mm

10 3 - 5 mm

가 3D - MR

, CT,

3D - VIBE

(one - stop shopping modality)

2D - GRE 3D -

VIBE 가

가 (MPR)

(PACS)

2D - GRE 3D - VIBE

가

3 4

가

, 3 - 4

가

가

가

3D - VIBE MR 2D -

FLASH MR

(cost effectiveness)

가 , 3D - VIBE MR 1

가

1. Rofsky NM, Weinreb JC, Bosniak MA, Libes RB, Birnbaum BA.

- Renal lesion characterization with gadolinium-enhanced MR imaging: efficacy and safety in patients with renal insufficiency. *Radiology* 1991;180:85-89
2. Yamashita Y, Miyazaki T, Hatanaka Y, Takahashi M. Dynamic MRI of small renal cell carcinoma. *J Comput Assist Tomogr* 1995; 19:759-765
3. Licht MR, Novick AC. Nephron sparing surgery for renal cell carcinoma. *J Urol* 1993;149:1-7
4. Provet J, Tessler A, Brown J, Golimbu M, Bosniak M, Morales P. Partial nephrectomy for renal cell carcinoma: indications, results and implications. *J Urol* 1991;145:472-476
5. Ciancio G, Politano VA, Ferrell S, Block NL. Renal parenchyma-sparing surgery as conservative treatment of renal cell carcinoma. *Br J Urol* 1994;74:422-430
6. Gschwend JE, Vogel U, Bader C, Mattfeldt T, Hautmann RE. Predictive value of magnetic resonance imaging and computerized tomography for conservative renal surgery in an ex vivo tumor enucleation study followed by step-sectioning. *J Urol* 1996;155: 451-454
7. Chernoff DM, Silverman SG, Kikinis R, et al. Three-dimensional imaging and display of renal tumors using spiral CT: a potential aid to partial nephrectomy. *Urology* 1994;43:125-129
8. Semelka RC, Shoenut JP, Kroeker MA, MacMahon RG, Greenberg HM. Renal lesions: controlled comparison between CT and 1.5 T MR imaging with nonenhanced and gadolinium-enhanced fat-suppressed spin-echo and breath-hold FLASH techniques. *Radiology* 1992;182:425-430
9. Rofsky NM, Bosniak MA. MR imaging in the evaluation of small (< or = 3.0 cm) renal masses. *Magn Reson Imaging Clin N Am* 1997; 5:67-81
10. Semelka RC, Hricak H, Stevens SK, Finegold R, Tomei E, Carroll PR. Combined gadolinium-enhanced and fat-saturation MR imaging of renal masses. *Radiology* 1991;178:803-809
11. Krestin GP, Steinbrich W, Friedmann G. Adrenal masses: evaluation with fast gradient-echo MR imaging and Gd-DTPA-enhanced dynamic studies. *Radiology* 1989;171:675-680
12. Huch Boni RA, Debatin JF, Krestin GP. Contrast-enhanced MR imaging of the kidneys and adrenal glands. *Magn Reson Imaging Clin N Am* 1996;4:101-131
13. Eilenberg SS, Lee JK, Brown J, Mirowitz SA, Tartar VM. Renal mass: evaluation with gradient-echo Gd-DTPA-enhanced dynamic MR imaging. *Radiology* 1990;176:333-338
14. Rofsky NM, Lee VS, Laub G, et al. Abdominal MR imaging with a volumetric interpolated breath-hold examination. *Radiology* 1999; 212:876-884
15. Choyke PL, Walther MM, Wagner JR, Rayford W, Lyne JC, Linehan WM. Renal cancer: preoperative evaluation with dual-phase three-dimensional MR angiography. *Radiology* 1997;205: 767-771
16. Heiss SG, Shifrin RY, Sommer FG. Contrast-enhanced three-dimensional fast spoiled gradient-echo renal MR imaging: evaluation of vascular and nonvascular disease. *RadioGraphics* 2000;20:1341-1352
17. Scattoni V, Colombo R, Nava L, et al. Imaging of renal cell carcinoma with gadolinium-enhanced magnetic resonance: radiological and pathological study. *Urol Int* 1995;54:121-127
18. Soyer P, Bluemke DA, Bliss DF, Woodhouse CE, Fishman EK. Surgical segmental anatomy of the liver: demonstration with spiral CT during arterial portography and multiplanar reconstruction. *AJR Am J Roentgenol* 1994;163:99-103
19. Carlson J, Crooks L, Ortendahl D, Kramer DM, Kaufman L. Signal-to-noise ratio and section thickness in two-dimensional ver-

- sus three-dimensional Fourier transform MR imaging. *Radiology* 1988;166:266-270
20. Glockner JF. Three-dimensional gadolinium-enhanced MR angiography: applications for abdominal imaging. *RadioGraphics* 2001;21:357-370
21. Du YP, Parker DL, Davis WL, Cao G. Reduction of partial-volume artifacts with zero-filled interpolation in three-dimensional MR angiography. *J Magn Reson Imaging* 1994;4:733-741
22. Gervais DA, McGovern FJ, Wood BJ, Goldberg SN, McDougal WS, Mueller PR. Radio-frequency ablation of renal cell carcinoma: early clinical experience. *Radiology* 2000;217:665-672
23. Miao Y, Ni Y, Bosmans H, et al. Radiofrequency ablation for eradication of renal tumor in a rabbit model by using a cooled-tip electrode technique. *Ann Surg Oncol* 2001;8:651-657
24. Duque JL, Loughlin KR, O'Leary MP, Kumar S, Richie JP. Partial nephrectomy: alternative treatment for selected patients with renal cell carcinoma. *Urology* 1998;52:584-590

J Korean Radiol Soc 2002;47:635 - 642

Contrast-Enhanced Three-Dimensional MR Imaging Using a Volumetric Interpolated Breath-hold Examination (VIBE): Clinical Utility in the Evaluation of Renal Tumors¹

Young Hwan Lee, M.D., Jeong Min Lee, M.D.², Chong Soo Kim, M.D.

¹Department of Diagnostic Radiology, Chonbuk National University Hospital, Chonbuk

²Department of Radiology, Seoul National College of Medicine and the Institute of Radiation Medicine, SNUMRC

Purpose: To compare, in terms of technical feasibility, image quality and clinical efficacy, contrast-enhanced three-dimensional (3D) MR imaging using volumetric interpolated breath-hold examination (VIBE) with two-dimensional gradient-echo MR imaging for the evaluation of renal masses.

Materials and Methods: Twenty-three patients with 25 renal masses underwent dynamic MR imaging using a 1.5-T MR system and the 3D VIBE, 2D fast low angle shot (FLASH), and combined fat saturation techniques after the injection of 20 ml of Gd-DTPA. We compared postcontrast 2D FLASH and 3D VIBE images with precontrast 2D FLASH images. For quantitative analysis, the signal-to-noise and lesion to kidney contrast-to-noise ratio of the images were calculated using the three different techniques. For qualitative analysis, two experienced radiologists analyzed the images in terms of artifacts, lesion conspicuity and delineation, and general image quality. Delineation of the anatomy of renal vasculature and pelvocalyceal systems on reconstructed 3D VIBE MIP images was also assessed.

Results: Quantitative analysis showed that the SNR of a renal mass was slightly higher at postcontrast 2D FLASH than at 3D VIBE imaging, and the SNR of renal cortex was higher at 3D VIBE than at postcontrast 2D FLASH imaging. The differences were, though, statistically insignificant ($p > 0.05$). The CNR of a renal mass was, however, significantly higher at 3D VIBE than at 2D FLASH imaging ($p < 0.05$). Qualitative analysis showed that general image quality was best at postcontrast 3D VIBE, followed by 2D FLASH and precontrast 2D FLASH imaging, and image artifacts were worst at post-contrast 2D FLASH image ($p < 0.05$). In terms of lesion conspicuity and delineation, 3D VIBE gave the best results and postcontrast images were better than precontrast ($p < 0.05$). Reconstructed angiographic and urographic images using the VIBE technique provided information about the anatomy of the renal vasculature and pelvocalyceal system.

Conclusion: 3D VIBE MR imaging offers comparable or superior image quality to 2D FLASH, and because it can provide angiograms and urograms may be more useful in the staging work-up of renal malignancies.

Index words : Kidney, MR
Kidney, neoplasms

Address reprint requests to : Jeong-Min Lee, M.D., Department of Radiology, Seoul National University Hospital,
28 Yongon-dong, Chongno-gu, Seoul 110-744, Korea.
Tel. 82-2-760-2514 Fax. 82-2-743-6385 E-mail: leejm@radcom.snu.ac.kr